



# Investigation on Dynamic Meshing Process and Factors Influencing Root Crack Propagation Trajectory of a Representative Aero-engine Gear Pair

Zhen Qu, Dianyin Hu, Rongqiao Wang

## ► To cite this version:

Zhen Qu, Dianyin Hu, Rongqiao Wang. Investigation on Dynamic Meshing Process and Factors Influencing Root Crack Propagation Trajectory of a Representative Aero-engine Gear Pair. 17th International Symposium on Transport Phenomena and Dynamics of Rotating Machinery (ISROMAC2017), Dec 2017, Maui, United States. hal-02392289

**HAL Id: hal-02392289**

**<https://hal.archives-ouvertes.fr/hal-02392289>**

Submitted on 3 Dec 2019

**HAL** is a multi-disciplinary open access archive for the deposit and dissemination of scientific research documents, whether they are published or not. The documents may come from teaching and research institutions in France or abroad, or from public or private research centers.

L'archive ouverte pluridisciplinaire **HAL**, est destinée au dépôt et à la diffusion de documents scientifiques de niveau recherche, publiés ou non, émanant des établissements d'enseignement et de recherche français ou étrangers, des laboratoires publics ou privés.

# Investigation on Dynamic Meshing Process and Factors Influencing Root Crack Propagation Trajectory of a Representative Aero-engine Gear Pair

Zhen Qu<sup>1</sup>, Dianyin Hu<sup>1,2,3\*</sup>, Rongqiao Wang<sup>1,2,3</sup>



## Abstract

The gear in an aero-engine experiences alternate loads therefore the stresses on gear root change significantly in meshing process. As a consequence, fatigue crack initiates on the gear root. This paper examined meshing process and crack propagation trajectory of the aero-engine gear based on explicit dynamics and linear elastic fracture mechanics. The crack on gear root affects meshing process and causes additional noise and vibration. The meshing impact and the peak of stress distribution of the gear pair is also magnified. Furthermore, the root crack propagation can cause the rim fracture and tooth fracture of gear system. The occurrence of rim fracture increases as the backup ratio (i.e., rim thickness divided by tooth height) decreases and also increases as the initial crack location is moved down the root of the tooth; the orientation of initial crack has little influence on crack propagation trajectory.

## Keywords

Dynamic meshing — Crack propagation trajectory—Gear—Finite element method

1. School of Energy and Power Engineering, Beihang University, Beijing, 100191, China;

2. Collaborative Innovation Center of Advanced Aero-Engine, Beijing 100191, China;

3. Beijing Key Laboratory of Aero-Engine Structure and Strength, Beijing 100191, China

\*Corresponding author: hdy@buaa.edu.cn

## INTRODUCTION

Gear transmission, which is widely used to transfer the torque and force between any two or more axles, is the most important form in mechanical drive. Main accessory systems of the engine, such as fuel system, lubrication system and hydraulic system, are all powered by the engine rotor through the gear transmission system. The tooth of the gear endures the fatigue loads (meshing force), which causes the fatigue crack on the root of the tooth during the meshing process.

Numerous studies on dynamic meshing process and the crack propagation trajectory of the gear have been carried out.

Hu analyzed the dynamic characteristic (time-varying meshing stiffness, acceleration, error transfer, mesh force, friction) of gear system with root crack using the lumped parameter dynamic model. [1-3] Wu S used the statistical methods to study the vibration response of the gear pair with simplified linear crack. [4] Although the dynamic meshing process of the crack gear is analyzed, the crack propagation path is not further considered.

Lewicki from fracture mechanics group of Cornell studied the influencing factors (initial position of the crack, initial angle of the crack, geometric construction of the gear and the rotational speed of the gear) of the crack propagation trajectory. [5-8] Liu simulated the trend of crack propagation of the maximum stress area of the gear tooth using ABAQUS. [9] Curà F calculate the impact of the initial position and angle of crack and the ratio of height and the thickness of tooth by the method of extend finite element method. [10]. Spievak L E investigated the crack trajectory prediction and fatigue life for a spiral bevel pinion using Finite Element Method. [11]

Based on the aforementioned analysis, this paper focuses on

a respective aero-engine gear pair in the accessory gearbox and makes the comprehensive consideration of dynamic meshing process and crack propagation trajectory.

## 1. METHODS

In the study of the dynamic meshing process of the gear pair with root crack, based on the method of explicit dynamics analysis, the time-varying parameters (the rotational speed, engaging force and Von Mises stress) of the cracked gear pair are calculated and compared with the healthy one. And the analyzing and processing these time-varying signals provides the basis to the diagnosis of the gear pair. If there appears initial crack on the root of gear tooth, it will grow during meshing process. The crack propagation trajectory differs on different initial condition and different gear design. So, using the method of finite element and the code of franc2d [12], the influencing factors (initial position, angle of the crack and backup ratio) of crack propagation trajectory and corresponding different fracture forms (tooth fracture and rim fracture) are carried out. The entire process of crack propagation is divided into several steps, and the angle ( $\theta$ ) of each crack propagation can be calculated by the following procedure. Firstly, with the method of J-integral [13][14] in the finite element analysis, the stress intensity factor and the stress distribution can be calculated using the code of franc2d.

$$J = \int_{\Gamma} [W \mathbf{dy} - \mathbf{T} \cdot \frac{\partial \mathbf{u}}{\partial \mathbf{x}} \mathbf{ds}] \quad (1)$$

$$W = \frac{1}{2} \int_0^{\epsilon_y} \sigma_y d\epsilon_y = \frac{1}{2} \sigma_y \epsilon_y \quad (2)$$

Equation(1) is the J-integral around the crack tip and  $W$  in equation(2) is energy density which can be got by the product of stress and strain.  $\mathbf{T}$  is the force acting on the integral boundary.

$$J = G = \frac{K^2}{E} \quad (3)$$

Because the result of J-integral is equal to the energy release rate  $G$  [15] in linear fracture mechanics, stress intensity factor  $K$  can be got according equation(3).  $E$  is elasticity modulus of material.

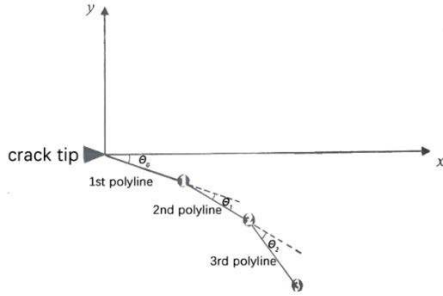


**Figure1.** The crack propagation trajectory of polylines

Then, the vertical direction  $\theta_i$  of the maximum circumferential stress around crack tip is regarded as the direction of crack propagation for the step  $i$  ( $i=1,2,\dots$ ). (Figure1.) Thirdly, the crack extends a tiny distance along  $\theta_i$  and the first polyline can be achieved. The codes continue to calculate the direction ( $\theta_{i+1}$ ) for the next step and the second polyline. By cycle computing, finally, the crack propagation trajectory can be obtained which is composed of these tiny polylines.

The following study of crack propagation trajectory prediction of the representative gear provides recommended design principles in order to prevent the occurrence of fracture failure of gears. In short, they can serve as the guidelines when conducting the failure prediction and fault diagnosis of gear system.

### 3. 2. The geometry model and mesh generation

The geometric parameters of gear pair are listed as follows.(Chart1.)

Chart 1. Geometric parameters of gear pair

	Driving gear	Driven gear
Teeth number $z$	31	40
Module $m$	2.54	
Pressure angle $\alpha$	20°	

The gear pair studied in this paper is rotated around z axis in the x-y plane. In order to save calculation time and improve the computational efficiency, the 2d gear model which is the projection on the x-y plane is used in the calculation. In analysis of dynamic meshing process and crack propagation trajectory, the 2d gear pair model(Figure2) and the 2d partial gear model(Figure3) with three teeth is used separately. In the FEM analysis, the elasticity modulus is 194GPa, the poisson ratio is 0.297 and the density is 7.86e-9t/mm<sup>3</sup>. Besides, the element type is plane stress element with midside node.

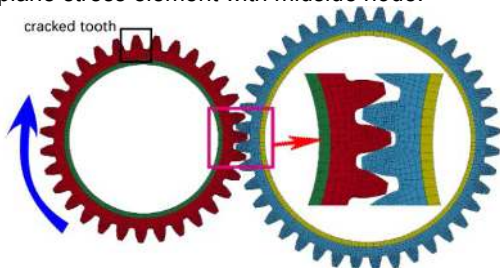


**Figure2.** 2d Model of Gear Pair

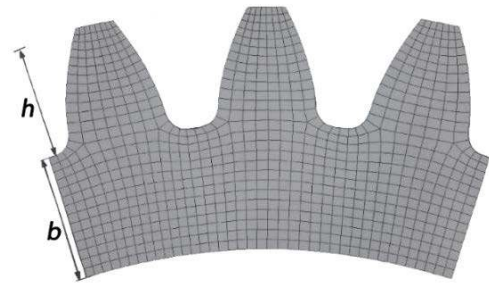


**Figure3.** 2d Partial Model(driving gear)

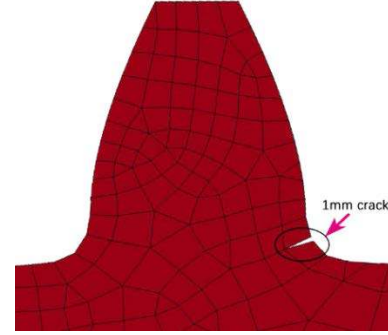


**Figure4.** Partial Magnification of the Cracked Tooth (driving gear)

In the process of generation of elements of the gear pair, each gear is divided into two parts. So the whole finite element model is divided into four parts shown in Figure2, driving gear part (red element part), driving gear rigid part (green element part), driven gear part (blue element part) and driven gear rigid part (yellow element part). The rigid element parts of gear pair which can not be deformed are only used to transfer velocity to the driving part and resistance torque to driven part. The crack on the tooth root (Figure4.) is generated by dividing one node on the root of gear tooth into two nodes and its length depends on the side length of the element on the driving gear.

### 3. Analysis of dynamic meshing process

#### 3.1 Contact dynamics method

During the process of gear meshing which involves impact and contact between gear teeth, the magnitude and direction of loads(engaging force) acting on the tooth change as time. When solving the contact problems, the penalty method is used for its simple principle, easy programming, low possibility of causing hourglass effect, less numerical noise and the high precision in the method of momentum conservation. [16]

$$f = k\delta \quad (4)$$

$$k = \frac{f_s KA^2}{V} \quad (5)$$

The penalty method assumes that there is linear spring between the contact points if they have penetrated each other and the spring force is expressed as Equation(4), where  $f$  is the spring force,  $k$  is the contact stiffness. The contact stiffness as Equation(5), where  $f_s$  is penalty factor(default value is 0.1),  $K$  is the bulk modulus of contact elements,  $A$  is elements contact dimension and  $V$  is elements contact volume.

The aim of dynamic analysis of meshing process is to compute the mechanical and time parameters of each time-step. The dynamic parameter of next time-step is related to the meshing state of pervious time-step. So on the basis of the previous meshing state, an incremental solution procedure can be used to solve the problem. First, we should determine the time step  $\Delta t$  in accordance with the reference [17] and the whole analysis of

meshing process can be dispersed into several time series(0,  $\Delta t, 2\Delta t, \dots, t + \Delta t, \dots T$ ). Second, time incremental algorithm is induced in the motion equation set on the concept of virtual displacement principle.(Equation6-9)

$$\begin{cases} [M]_g {}^{t+\Delta t}\ddot{u}_g + [C]_g {}^{t+\Delta t}\dot{u}_g + {}^t[K]_g u_g = \\ {}^{t+\Delta t}[F]_g^L + {}^{t+\Delta t}[F]_g^C - {}^t[F]_g \\ [M]_p {}^{t+\Delta t}\ddot{u}_p + [C]_p {}^{t+\Delta t}\dot{u}_p + {}^t[K]_p u_p = \\ {}^{t+\Delta t}[F]_p^L + {}^{t+\Delta t}[F]_p^C - {}^t[F]_p \end{cases} \quad (6)$$

$${}^{t+\Delta t}u_g = \begin{bmatrix} {}^{t+\Delta t}x_1 \\ {}^{t+\Delta t}y_1 \\ {}^{t+\Delta t}z_1 \end{bmatrix} - \begin{bmatrix} 0 \\ 0 \\ 0 \end{bmatrix} \begin{bmatrix} x_1 \\ y_1 \\ z_1 \end{bmatrix}; {}^t u_g = \begin{bmatrix} {}^t x_1 \\ {}^t y_1 \\ {}^t z_1 \end{bmatrix} - \begin{bmatrix} 0 \\ 0 \\ 0 \end{bmatrix} \begin{bmatrix} x_1 \\ y_1 \\ z_1 \end{bmatrix} \quad (7)$$

$${}^{t+\Delta t}u_p = \begin{bmatrix} {}^{t+\Delta t}x_2 \\ {}^{t+\Delta t}y_2 \\ {}^{t+\Delta t}z_2 \end{bmatrix} - \begin{bmatrix} 0 \\ 0 \\ 0 \end{bmatrix} \begin{bmatrix} x_2 \\ y_2 \\ z_2 \end{bmatrix}; {}^t u_p = \begin{bmatrix} {}^t x_2 \\ {}^t y_2 \\ {}^t z_2 \end{bmatrix} - \begin{bmatrix} 0 \\ 0 \\ 0 \end{bmatrix} \begin{bmatrix} x_2 \\ y_2 \\ z_2 \end{bmatrix} \quad (8)$$

$$u_g = {}^{t+\Delta t}u_g - {}^t u_g; u_p = {}^{t+\Delta t}u_p - {}^t u_p \quad (9)$$

Subscripts  $g$  and  $p$  are for driving gear and driven gear. Matrix  $[M]$ ,  $[K]$  and  $[C]$  are for mass matrix, stiffness matrix and dumping matrix.  $\ddot{u}$ ,  $\dot{u}$  and  $u$  are for the acceleration, velocity and displacement of the element node. The superscripts  $L$  and  $C$  of  $[F]$  are for the external nodal load and nodal contact force.  ${}^t[K]_g$  and  ${}^t[K]_p$  are respectively stiffness matrix of the driving gear and driven gear at the reference mement which is determined by the position and configuration of gear pair.  ${}^t F_p$  and  ${}^t F_g$  are the internal force vector of driving gear and driven gear at  $t$ .  $u_p$  and  $u_g$  are incremental nodal displacement of driving and driven gear.  ${}^t \dot{u}$  and  ${}^t u$  ( $t=0$ ) can be determined by the initial condition of the gear engagement. According the penalty method, the nodal contact force vector can be written as

$$\begin{aligned} {}^{t+\Delta t}F_C^p &= -f_s N_C \left( -\mu \frac{u_1}{u_T} {}^{t+\Delta t}e_1 - \mu \frac{u_2}{u_T} {}^{t+\Delta t}e_2 + {}^{t+\Delta t}e_N \right) \\ \bullet \left( {}^{t+\Delta t}e_N N_C u_C + {}^t g_N \right) &= F_{T1}^p + F_{T2}^p + F_N^p \end{aligned} \quad (10)$$

where  $N_C$  is interpolation function,  $\mu$  is coefficient of sliding friction,  $u_T$  is tangential displacement increment,  $u_1$  and  $u_2$  are tangential displacement increment of the two directions respectively,  ${}^t g_N$  is normal distance of the two contact point at  $t$ ,  $u_C$  is relative normal distance of contact point from  $t$  to  $t + \Delta t$ ,  $F_{T1}^p$  and  $F_{T2}^p$  are tangential components of equivalent contact force of two directions and  $F_N^p$  is normal component of the equivalent contact force. Center difference method is used to solve Equation(6) by substituting  ${}^{t+\Delta t}u$  and  ${}^{t+\Delta t}\dot{u}$  expressed by Equation(11) and Equation(12). Then Equation(13) which is recursion formula of  ${}^{t+\Delta t}u$  can be got.

$${}^{t+\Delta t}u = {}^t u + {}^t \dot{u} \Delta t + \frac{1}{2} {}^t \ddot{u} \Delta t^2 \quad (11)$$

$${}^{t+\Delta t}\dot{u} = {}^t \dot{u} + \frac{1}{2} ({}^t \ddot{u} + {}^{t+\Delta t} \ddot{u}) \Delta t \quad (12)$$

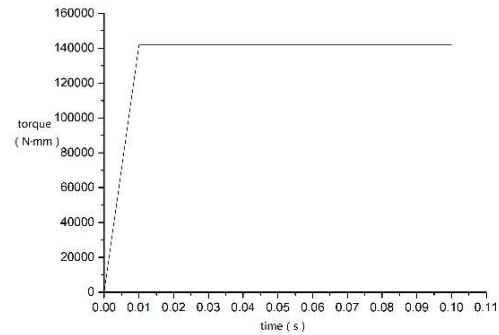
$${}^{t+\Delta t}\ddot{u} = \frac{{}^{t+\Delta t}[F]_L + {}^{t+\Delta t}[F]_C - {}^{t+\Delta t}[F] - ({}^t \dot{u} + \frac{1}{2} {}^t \ddot{u} \Delta t)[C]}{[M] + \frac{1}{2} \Delta t [C]} \quad (13)$$

$${}^{t+\Delta t}[F] = {}^t [F] + {}^t [K] u \quad (14)$$

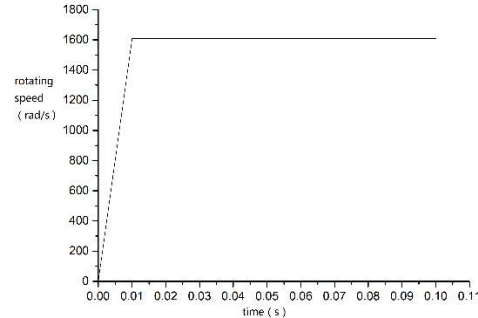
Through equation (11) and (13),  ${}^{t+\Delta t}u$  and  ${}^{t+\Delta t}\ddot{u}$  can be figured up and then  ${}^{t+\Delta t}\dot{u}$  can be calculated subsequently by Equation(12). Then the internal force, contact force and nodal force of next increment time step can be calculated.

### 3.2 The analysis of the meshing calculation result

The loading curves are shown in Figure5(a) and (b).The rotating speed(1608.6rad/s) is applied on the driving gear rigid part and the burden torque (141900N·mm) is applied on the driven gear rigid part. The value of rotating speed and torque match actual parameters of a genuine engine. Automatic surface-to-surface contact is selected as the contact principle.



(a) Torque



(b) Rotating Speed

Figure5. Loading Curve

The result of rotating speed of the driven gear, the engaging force and the element contact stress changing over time is analyzed in the following characters.

#### 3.2.1 Analysis of the rotating speed

The rotating speed applied on driving gear rigid part starts at zero and increases linearly to 1608.8 rad/s within 0.01 second shown as Figure5.(b). The rotating speed of the driven gear is 1246.7rad/s which can be calculated through the gear ratio. And its rotating speed changing over time is shown in Figure6. The finite element model with a 1mm crack shown in Figure4. is used in the dynamic calculation and the time-rotating speed curve which is shown in Figure7 is quite different from the curve shown in Figure6



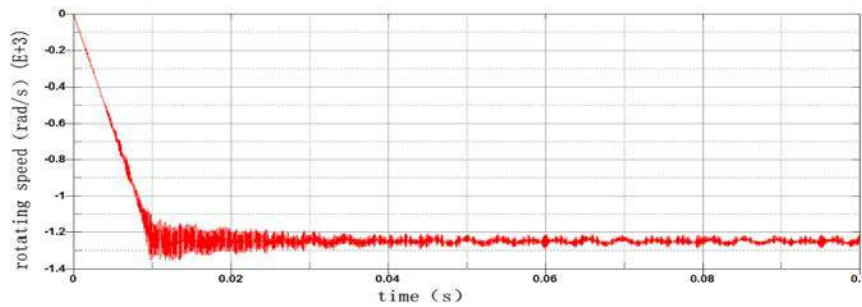


Figure6. Rotating Speed of the healthy Gear

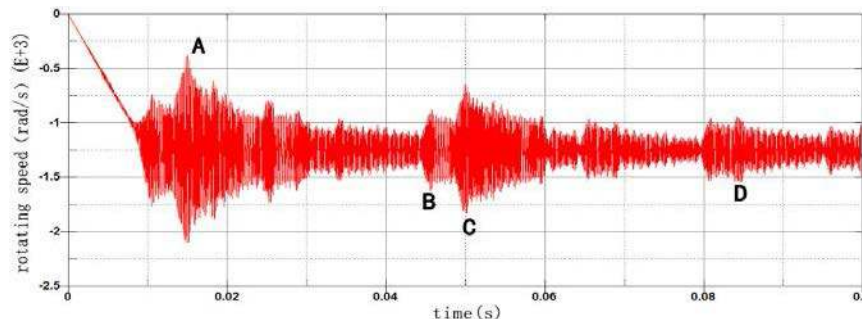
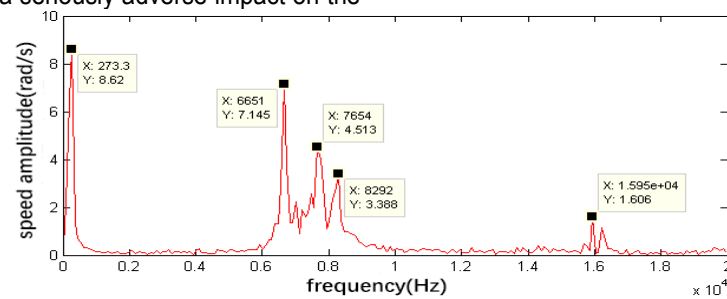


Figure7. Rotating Speed of cracked gear pair

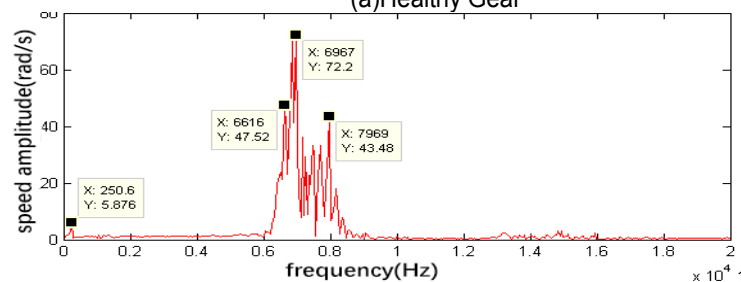
The trends of the output rotating speed of both the healthy gear and the cracked one coincide with the input rotating speed of the driving gear (Figure 5). After 0.01 second the rotating speed of the driving gear reaches the setting speed linearly and the rotating speed of the driven gear fluctuates around the theoretical rotating speed. By comparing the curve in Figure 6 and Figure 7, we can see that the fluctuation amplitude of the rotating speed of the healthy driven gear is almost stable after 0.04 second and the cracked gear is 0.065 second. The maximum rotation speed fluctuation amplitude of the cracked gear is about 750 rad/s (point A in Figure 7) which is almost ten times larger than the healthy one (75 rad/s) during meshing process. So, it can be seen that the vibration shock of the cracked gear pair is significantly enhanced in the process of engaging. Affected by the increase of vibration amplitude, the gear pair inevitably produces the abnormal noise during the meshing process, which has a seriously adverse impact on the

normal stable transmission of gear pair.

The time domain data of 0.08 second to 0.1 second in Figure 6 and Figure 7 which have been stable are subjected to Fourier transform to obtain the curve in frequency domain shown in Figure 8(a) and (b) which is calculated by LS-DYNA. The first peak on the left of the curve in Figure 8(a) and (b) corresponds to the rotational frequency which is 298 Hz ( $1608.8/2\pi$ ) theoretically. The peaks of the middle part of the curve corresponds to the meshing frequency which is 7936.67 Hz in theory and the possible natural frequency of the gear. The rightmost peak corresponds to the second frequency of the meshing frequency. Because of the crack on the root of the gear the proportion of the meshing frequency and the vibration amplitude is significantly changed. The crack on the root of the gear pair that causes damage to the structure of the gear pair intensifies the impact in the meshing process, which causes abnormal noise and vibration and greatly shorten the service life of the gear pair



(a) Healthy Gear



(b) Cracked Gear

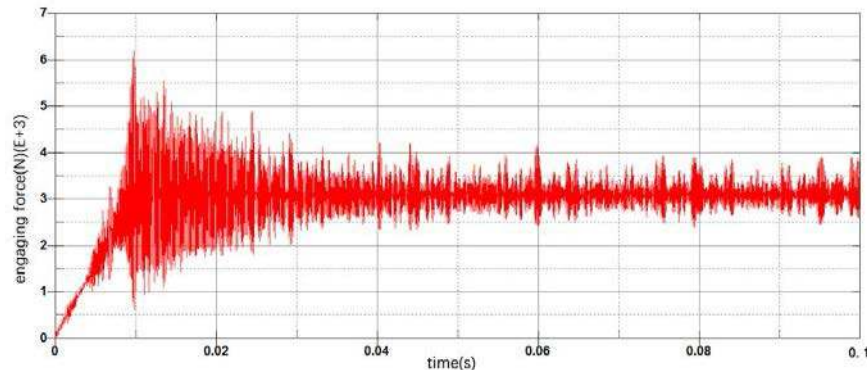
Figure8. Amplitude-versus-frequency Curve

### 3.2.2 Analysis of the engaging force and the element contact stress

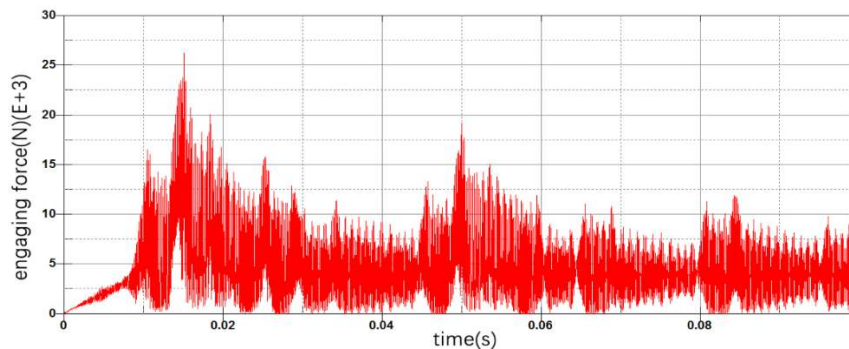
The output of contact force and the node force come from the result of the LS-DYNA calculation, the engaging force is extracted shown in Figure9.

In the initial stage (0.01s-0.02s) of high-speed meshing, the curve of the meshing force fluctuates greatly with time, and it is obvious that there is an impact. And with the time goes by, the fluctuation amplitude of the engaging force decreases gradually. After about 0.04 seconds in Figure9(a) and 0.065 seconds in Figure9(b), the mesh enters the stable transmission phase,

which coincides with the result of the rotating speed in Figure8. The engaging force of the healthy driving gear is constant positive, which means that there is only unilateral meshing which means that only one side of the tooth is in the contact situation during the process but the engaging force of the cracked gear has both positive and zero value, based on which the engaging force of the driving gear should be decomposed into the x-direction (parallel to the direction of line of centers) and y-direction (perpendicular to the direction of line of centers) shown in Figure10.



(a) Healthy Driving Gear

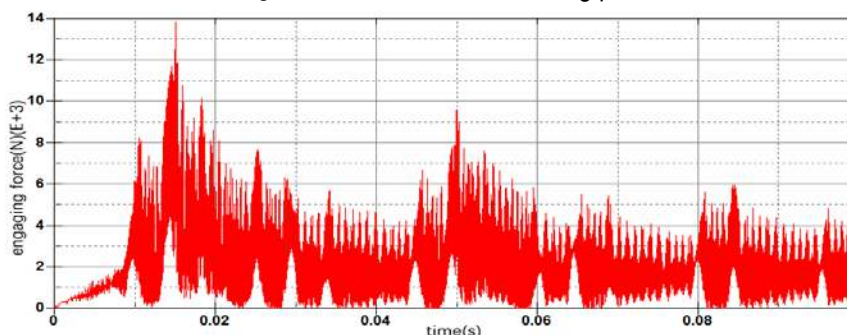


(b) Cracked Driving Gear

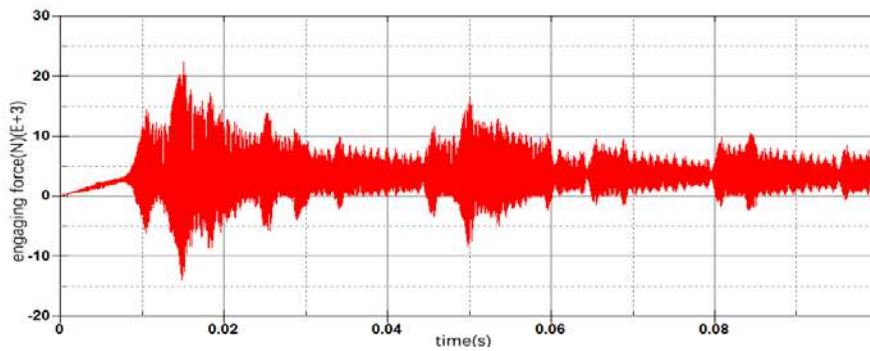
Figure9. Engaging Force

Compared with the meshing process of the healthy gear pair, the moment when the cracked gear pair enters the stable speed fluctuation which means that the vibration amplitude of speed is almost constant is obviously pushed backward. Moreover, the maximum peak-to-peak value of the fluctuation of engaging force of the cracked gear is 25kN, which is much larger than that of 5kN of healthy gear pair. The x-direction of engaging force shown in Figure10(a) exists both positive value and zero value indicates that there is a phenomenon of tooth off which means that there is a moment when the tooth of the gear is not in the

contact condition in meshing process. The x-direction of the engaging force shown in Figure10(b) exists positive, zero and negative value indicates that there are not only unilateral and 'tooth off' meshing but also 'bilateral impact' meshing which means that both the two sides of one tooth have an impact on the adjacent sides of other tooth. The cause of the occurrence of tooth off and bilateral impact is that the ability of gear teeth to resist bending deformation is reduced and the bending stiffness of the gears is also reduced after the initiation of crack during the meshing process.



(a) X-direction

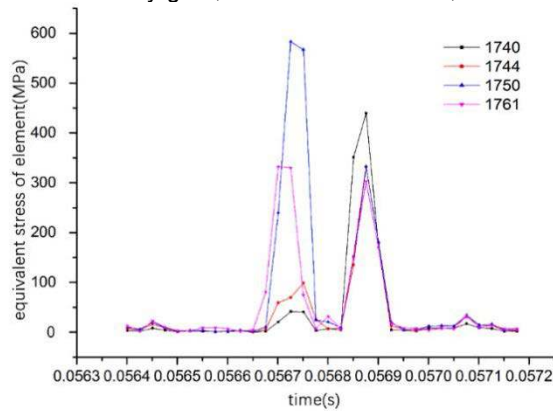


(a) Y-direction

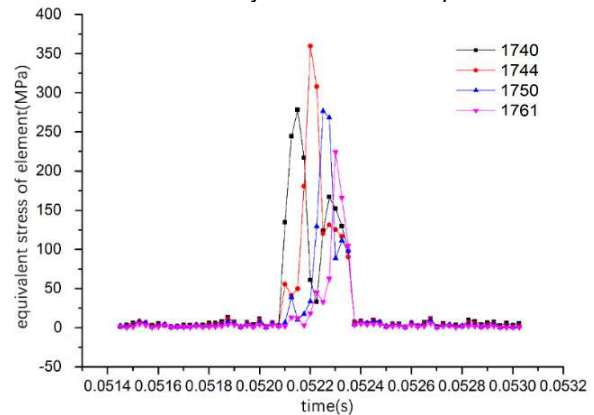
Figure10. Decomposition of the Engaging Force of the Cracked Gear

The equivalent stress(Von Mises stress) of four chosen elements on the contact surface of gear tooth changing over time is shown in Figure11 during the meshing process of one tooth. By comparing (a) and (b) in Figure11, obviously, there are two peaks on the curve of the cracked gear while only one on the curve of healthy gear, which indicates that ,because of the

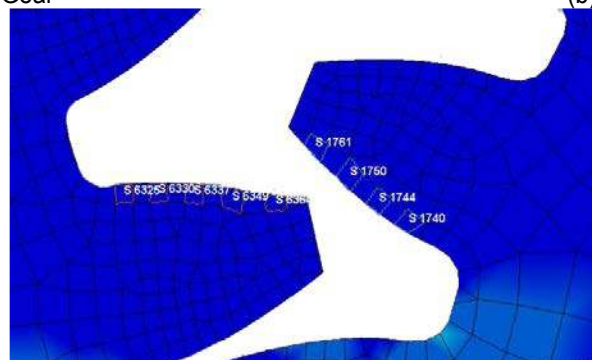
crack on the root of the gear intensifying the vibration shock, bilateral impact occurs on the cracked gear pair while there is only unilateral meshing on the healthy gear pair. The maximum equivalent contact stress (Von Mises stress) of cracked gear is 660MPa, which is obviously larger than that of the healthy gear and this is also caused by the increased impact of cracked gear.



(a) Healthy Gear



(b) Cracked Gear



(c) Finite element model

Figure11. Equivalent Stress of Elemen

#### 4. Analysis of the crack propagation trajectory

The initial crack on the root of gear will propagate during the meshing process. At the initial propagation stage, the crack on the gear is so tiny that could not cause the catastrophic failure of gear system. Acceleration sensor can be used to monitor data of the gear system and determine whether there is a failure in the system according the analysis of previous chapter. However, if the initial crack is not monitored at the initial propagation stage and the gear system continues to work, the initial crack will continue to propagate in different directions and cause the rim fracture or tooth fracture. The rim fracture leads to more serious failure in the gear system than tooth fracture, so it is necessary to analyze the possible crack propagation trajectory.

##### 4.1 Determination of load and boundary conditions

The literature [18] combined the numerical simulation and experimental verification to draw the conclusion that in the simulation of the tooth root crack propagation trajectory, the crack propagation path can be obtained sufficiently accurately with a static load applied to the gear at the position of the highest meshing point instead of the moving dynamic load. The value of the equivalent static load is determined according to the actual conditions of the gear pair.

$$T = 9550 \frac{P}{N} \quad (15)$$

The input torque (T) of the driving gear is 184.9N·m by equation (6) , where the rotating speed (N) is 15361.3 r/min and input power (P) of the driving gear is 297.5kw. The transmission

ratio (i) is 31/40 and the transmission efficiency is 0.99. The input torque  $T_{input}$  can be calculated.  $T_{input} = 141.9 \text{ N}\cdot\text{m}$ . The nominal circumference force ( $F_t$ ) and nominal radial force ( $F_r$ ) of the gear tooth is obtained by equation (7), (8) and (9).

$$d = (z + 2h_a^*) \cdot m \tag{16}$$

$$F_t = \frac{2000T_{input}}{d} \tag{17}$$

$$F_r = F_t \cdot \tan 20^\circ \tag{18}$$

The force is applied on the point A and the fix constraint is applied to the lower, left and right sides of the rim of the partial gear model. (Figure12) Experiments on the finite element model of the whole gear and partial gear pair with three tooth have been done, which justifies that the constraints used on the partial gear pair has the same result with whole gear.

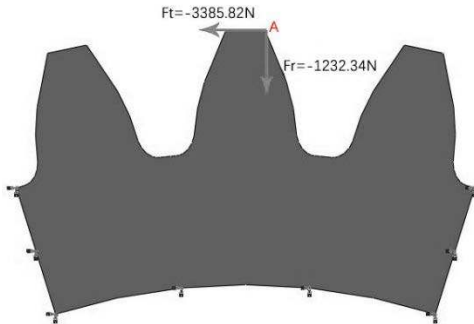


Figure12. Load and Boundary Condition

#### 4.2 Influencing factor of crack propagation trajectory

The angle of crack propagation is obtained for each sub-step by calculating the stress intensity factor of crack tip. The local meshes of the crack region can be redivided by the 'element addition and deletion' in the FRANC program and the program doesn't stop until the crack propagation trajectory reaches the boundary of the finite element model. Finally, the crack propagation trajectory can be obtained shown in Figure13. The simulation results of the crack propagation trajectory coincide with the simulated results in the literature [2] and the experimental results in literature [18] show the accuracy of the numerical simulation of the FRANC program in literature [2].

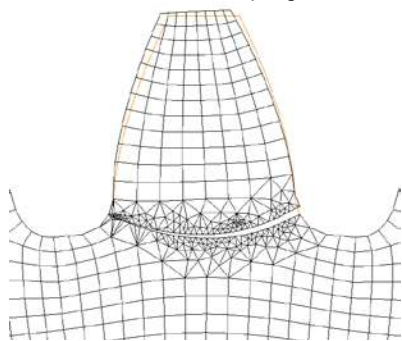
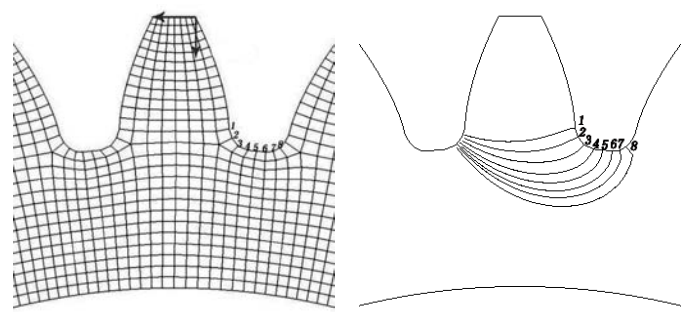


Figure13. Crack Propagation Trajectory

##### 4.2.1 Influence of initial crack location on crack propagation trajectory

The initial crack is inserted at the root of the gear model from point 1 to point 8 shown in Figure14(a). The initial crack length is set to 0.3mm along the direction of the element. The crack is formed using the same method with finite element model in the dynamic calculation, but the length is shorter because the element size of the partial model with three teeth is smaller in order to obtain preciser crack propagation trajectory.



(a)Initial Crack Location (b)Crack Propagation Trajectory

#### Figure14. Influence of the Initial Crack Location on Crack Propagation Trajectory

The simulation of 8 crack propagation trajectories which is integrated into one figure is completed using the FRANC program 8 times shown in Figure14(b). The length of the crack trajectory in the rim region is gradually increased as the initial crack position moves down, and all the fracture form is the tooth fracture.

##### 4.2.2 Influence of initial crack orientation on crack propagation trajectory

In the process of gear processing, there are subtle scratches and the concentration of notch stress on the surface of the material and the corrosion of the working environment. When the local stress concentration exceeds the breaking strength, the atomic bond breaks and causes the initial fatigue crack in different directions on the surface of the material. The difference of the initial direction of the crack has a certain impact on the crack propagation trajectory.

The gears are subjected to alternating loads during the working process and the root is the position of stress concentration where there are the dangerous sections. The position of the dangerous section is determined by many kinds of methods. In this paper, the Hofer 30° Hazard section method[19] is used. According to the results of a large number of gears opto-elastic experiments, the tangent points (point A and point B in Figure 16) are obtained by drawing the line tangent to the tooth profile at a 30° angle with the centerline. The position of connection line between point A and point B is regarded as the position of the dangerous section of the gear.

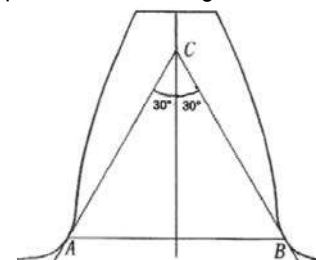


Figure16. Position of the Dangerous Section

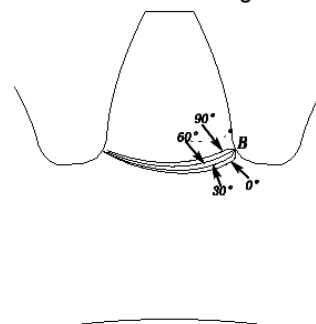
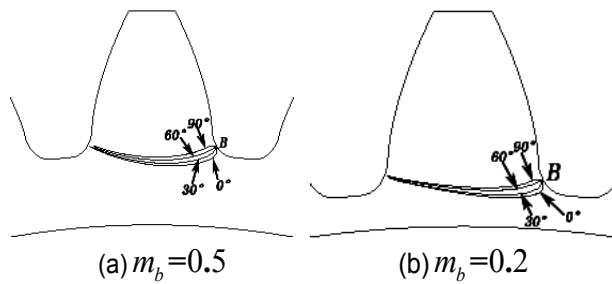


Figure17. Crack Propagation Trajectory( $m_b = 1$ )





**Figure18.** Crack Propagation Trajectory of Different Initial Orientation

In order to study the influence of the initial crack angle on the crack propagation trajectory, the initial crack location is selected at the point B on the dangerous cross section, and the initial cracks are along the four directions of  $0^\circ$ ,  $30^\circ$ ,  $60^\circ$  and  $90^\circ$  with the vertical direction respectively. The initial crack length is 0.3mm and the  $m_b$  is 1. The calculated four crack propagation trajectories are integrated in one figure shown in Figure17. When  $m_b$ , whose value is the ratio of b and h shown in Figure.3 is changed(Figure18), the crack propagation trajectories is basically the same as those in Figure17. Crack propagation causes the tooth fracture, so the influence of the initial crack orientation on the crack propagation path can be used as the secondary design reference factors.

#### 4.2.3 Influence of backup ratio on crack propagation trajectory

From the results of previous chapter, it can be deduced that when the rim thickness is thinned, the crack propagation may lead to rim fracture. When the backup ratio ( $m_b$ ) is 0.5 and 0.2, the crack propagation trajectory can be calculated with the same method and the result is shown in Figure19.

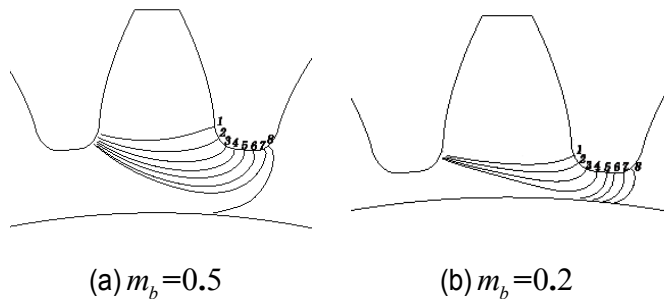


**Figure19.** Influence of Backup Ratio on Crack Propagation Trajectory

The crack propagation results of point 8 in Figure19(a) and point 5,6,7,8 in Figure19(b) are rim fracture, which verify the above inference. With the thinning of the rim thickness, the form of tooth fracture caused by crack propagation is more likely to occur at rim, which causes a more serious catastrophic accident in the entire gear system compared with tooth fracture. For gears in the gearbox of aeroengine accessory gears, gear failure can lead to failure of the hydraulic system, the oil system, and the electronic control unit, which may cause the consequences of the crash. Therefore, in the process of design and structural optimization of the gears, the backup ratio should first be considered to ensure the safe and reliable operation of the gear system.

## 5. Conclusion

Based on the finite element program, this paper completes the dynamics simulation of the gear meshing and the prediction of crack propagation trajectory in the actual working condition,

which provides the basis for the fault prediction and structural design of the gears.

The following conclusions are obtained from the study of this paper.

(1)The speed of the cracked gear fluctuates greater than that of the healthy one and is not easy to enter stable meshing stage. The crack changes the frequency domain characteristic of the rotating speed, which produces additional abnormal vibration and noise in meshing process.

(2)The crack on the root of the gear affect the stiffness of the gear, which can cause additional bilateral impact and disengagement. This leads to an increase in the instantaneous fluctuation of the engaging force, which can cause additional damage to the gear system.

(3) The position of the initial crack has a great influence on the crack propagation trajectory of the gear. The possibility of occurrence of rim fracture increases as the initial crack position moves down along the tooth root.

(4) The backup ratio of the gear structure also has a large effect on the crack propagation trajectory, and the possibility of occurrence of rim fracture is significantly increased with the decrease of backup ratio.

(5) The direction of the initial crack has little effect on the crack propagation trajectory, which can be used as a secondary reference factor in the design and optimization of the gear to ensure the safe and reliable operation of the gear system.

## ACKNOWLEDGMENTS

The present work is the result of all joint efforts. I would like to express my deep gratitude to Professor Dianyin Hu and Professor Jianjun Wang, who helped me modify the paper. Also, I would like to express my sincere gratitude to all the classmates who have discussed with me. Their instructions and suggestions have helped broaden my horizon.

Last but not least, I would like to express my special thanks to my parents, whose care and support motivate me to move on.

## REFERENCES

- [1] Xinpeng Hu, Xi Wu, Jixin Wang, Jim Meagher. Fault Detection of Gears with Different Root Crack Size Using Wavelet[C], Proceedings of the ASME 2015 International Design Engineering Technical Conferences & Computers and Information in Engineering Conference IDETC/CIE 2015, August 2-5, 2015, Boston, Massachusetts, USA.
- [2] Xinpeng Hu, Jingwen Yan, Yan Liu, et al. Influence of Different Gear Generation Methods on Contact Stress Analysis of Spur Bevel Gears in PSD[J]. Applied Mechanics and Materials, 2014, 448: 3476-3480.
- [3] Jixin Wang, Long Kong, Bangcai Liu, Xinpeng Hu, et al. The Mathematical Model of Spiral Bevel Gears-A Review[J]. Strojniški vestnik-Journal of Mechanical Engineering, 2014, 60(2): 93-105.
- [4] Wu S, Zuo M J, Parey A. Simulation of Spur Gear Dynamics and Estimation of Fault Growth[J]. Journal of Sound & Vibration, 2008, 317(3-5):608-624.
- [5] Lewicki D G. Gear Crack Propagation Path Studies -

Guidelines for Ultra-Safe Design [J]. Journal of the American Helicopter Society, 2001.

[6] Lewicki D G. Effect of Speed (Centrifugal Load) on Gear Crack Propagation Direction [J]. Effect of Speed on Gear Crack Propagation Direction, 2001.

[7] Lewicki D G, Ballarini R. Rim Thickness Effects on Gear Crack Propagation Life [J]. International Journal of Fracture, 1997, 87(1):59-86.

[8] Lewicki D G. Crack propagation studies to determine benign or catastrophic failure modes for aerospace thin-rim gears [D]. Case Western Reserve University, 1995.

[9] Liu Shuang, Zhu Rupeng. Simulation on propagation of Involute Gear Tooth Based on ABAQUS [J]. Journal of Nanjing University of Aeronautics and Astronautics, 2011, 43(1):59-68.

[10] Curà F, Mura A, Rosso C. Investigation about crack propagation paths in thin rim gears [J]. Frattura Ed Integrità Strutturale, 2014, 30(30):446-453.

[11] Spievak L E, Wawrzynek P A, Ingraffea A R, et al. Simulating fatigue crack growth in spiral bevel gears[J]. Engineering Fracture Mechanics, 2003, 68(1):53-76.

[12] Wawrzynek P, Ingraffea A. FRANC2D: A two-dimensional crack propagation simulator. Version 2.7: User's guide[J]. 1994.

[13] G. P. Cherepanov, The propagation of cracks in a continuous medium, Journal of Applied Mathematics and Mechanics, 31(3), 1967, pp. 503–512.

[14] J. R. Rice, A Path Independent Integral and the Approximate Analysis of Strain Concentration by Notches and Cracks, Journal of Applied Mechanics, 35, 1968, pp. 379–386.

[15] Rice J R. Fracture Mechanics[J]. Applied Mechanics Reviews, 1985, 38(10):1271-1275.

[16] Jinze Bai. LS DYNA3D theory foundation and example analysis. [M] Science Press,2005.

[17] Yongjun Wu. Contact Finite Element Analysis and Application Study on Dynamic Meshing Characteristics of Gear Transmission System[D]. Beihang University,2012.

[18] Lewicki D G, Handschuh R F, Spievak L E, et al. Consideration of Moving Tooth Load in Gear Crack Propagation Predictions[J]. Journal of Mechanical Design, 2000, 123(1):118-124.

[19] Jiaguo Xue. The calculation of the dangerous cross section of gear teeth based on conjugate surface principle [J]. Journal of Anhui University of Technology and Science(Natural Science), 1992(2):82-90. |